Circ_0004913 sponges miR-1290 and regulates FOXC1 to inhibit the proliferation of hepatocellular carcinoma

Yabin Yu
Huaian First People's Hospital
Suyang Han
Huaian First People's Hospital
Meng Li
Huaian First People's Hospital
Yan Song
Huaian First People's Hospital
fuzhen qi (qifuzhen2017@163.com)
Department of Hepatobiliary Surgery, The Affiliated Huaian No.1 People's Hospital of Nanjing Medical University https://orcid.org/0000-0001-9290-7694

Primary research

Keywords: Circ_0004913, miR-1290, FOXC1, Hepatocellular carcinoma

DOI: https://doi.org/10.21203/rs.3.rs-36547/v2

Abstract

Circ_0004913, miR-1290, FOXC1, Proliferation,Hepatocellular carcinoma.

1. Introduction

Accounting for approximately 90% of primary liver cancer, Hepatocellular carcinoma (HCC) is the third leading cause of cancer-related deaths in the world [1, 2]. Chronic hepatitis B virus (HBV), hepatitis C virus (HCV), heavy alcohol consumption and diabetes are the main risk factors for HCC [3]. There are currently several treatments for HCC, including surgical resection, chemoradiation, and liver transplantation. Sometimes, hepatocellular carcinoma requires a multidisciplinary treatment to get the best results [4]. However, the five-year overall survival rates of patients with HCC remain low, largely because of metastasis and recurrence [5]. In order to improve the diagnosis and prognosis of HCC patients, it is particularly critical to discover and identify new targets for precise treatment.

Circular RNAs (circRNAs) are a new type of non-coding RNAs, characterized by continuous covalent closed loop without 5'-cap structure or 3'-poly A tail, and considered as a by-product of splicing error [6]. Aberrant expression of circRNAs have also been shown to be associated with the initiation and development of various diseases, including cancers [7]. For example, circRNA FARSA promoted colorectal cancer cell growth, while circRNA UBAP2 increased SEMA6D expression to enhance cisplatin resistance in osteosarcoma [8, 9]. Various circRNAs exist in mammalian cells and regulate a broad range of biological processes through various mechanisms, including sponging of microRNAs (miRNAs) [10]. CircRNA circ_0054537 could sponge miR-130a-3p to promote the progression of renal cell carcinoma through regulating cMet pathway, and circ_0008532 promotes bladder cancer progression by regulation of the miR-155-5p/miR-330-5p/MTGR1 axis[11, 12]. However, the role of circ_0004913 in cancer is poorly understood.

Based on the information in the circbase database, circ_0004913, encoded by the TEX2(Testis expressed 2) gene, is located on chromosome chr17: 62248459-62265775 and about 495 bp [13]. In the HCC microarray data of GEO, the down-regulated circ_0004913 was selected as the research object. We hypothesized that circ_0004913 is involved in the malignant process of HCC and conducted a series of *in vitro* proliferation-related experiments. Circ_0004913 could significantly inhibit the proliferation of HCC cells *in vitro* and arrest more HCC cells in G1 phase. Circ_0004913 could also up-regulate the expression of FOXC1 (Forkhead box C1) in HCC cell line by interacting with miR-1290. These findings provide a new perspective into the function of circ_0004913 and highlight the potential of developing HCC treatments.

2. Materials And Methods

2.1 Microarray analysis

A comprehensive database of gene expression (GEO, http://www.ncbi.nlm.nih.gov/geo), which is a public repository for archiving and distributing microarrays for free, was screened. GSE97332 and GSE94508

were selected, and the “limma” package was used to analyze differences in gene expression between tumor and non-tumor tissues [14, 15]. CircRNAs with adjusted P<0.05 and |Log FC|>1 were considered as significant dysregulated circRNAs.

2.2 Patients

A total of 50 HCC patients who underwent surgical treatment in our hospital were enrolled from June 2012 to June 2015. The main screening criteria include: (1) histological diagnosis of primary HCC; (2) receiving surgical resection; (3) not receiving chemotherapy or radiotherapy before surgery; (4) complete preoperative tumor characteristics. In addition, this study Patients with relapsed or secondary HCC and a history of malignant tumors were excluded. The study was approved by the hospital's ethics committee. All patients or their families provided written informed consent.

2.3 Cell lines

Human HCC cell lines Hep3B, HepG2, SMMC-7721, and Huh-7, and the human normal liver cell line (LO2) were purchased from the Chinese Academy of Sciences (Shanghai, China) and were cultured in Dulbecco’s modified Eagle’s medium (DMEM; Gibco, California, USA) supplemented with 10% fetal bovine serum (Gibco) and antibiotics (100 U/ml penicillin G and 100 mg/ml streptomycin) at 37 °C in a humidified atmosphere with 5% CO_2.

2.4 QRT-PCR

Total RNA was isolated with TRIzol Reagent ((Beyotime, Shanghai, China)) following the manufacturer’s instruction. Then, 1 μg total RNA was reversed into 20 μl complementary DNA (cDNA) with First Strand cDNA Synthesis Kit (Takara, Tokyo, Japan). QRT-PCR was conducted using SYBR Green Master Mix II (Takara) on ABI7900 system (Applied Biosystems, CA, USA) in line with the manufacturer’s procedure. Circ_0004913, miR-1290, TEX2 and FOXC1 mRNA expression was determined using the $2^{-\Delta\Delta CT}$ method. A P-value < 0.05 denotes a statistical significance. GAPDH and U6 were used as internal controls for circRNA and miRNA, respectively. All primers were purchased from GenePharma (Shanghai, China). The primer sequences are as follows: Circ_0004913: Forward: 5'-TACGTTGATCACCAAGGGCT-3', Reverse: 5'-CTTCTGCTTTGGCTGTGACA-3'; miR-1290: Forward: ACACTCCAGCTGGGTGGATTTTTGGATC, Reverse: CTCAACTGGTGTCGTGGAGTCGGCAATT; FOXC1: Forward: 5'- AAAAAATTGGAGGCTGCTT-3', Reverse: 5'-CCAAAGAAAAATCCCCACA-3'; GAPDH: Forward: 5'-AAGGTGAAGGTCGGAGTCA-3', Reverse: 5'-GGAAGATGGTGATGGGATTT-3'; U6: Forward: 5'-CTCGCTTCGGCAGCACATATACT-3', Reverse: 5'-ACGCTTCACGAATTTGCGTGTC-3'.

2.5 RNase R treatment assay

2 μg RNA and 6 units of RNase R (Geneseed Biotech, Guangzhou, China) were added together to incubate for 20 min at 37 °C. Subsequently, circ_0004913 and TEX2 mRNA expression was detected through qRT-PCR.

2.6 Subcellular localization

The subcellular localization of circ_0004913 was detected using the PARIS Kit (Invitrogen, CA, USA) in accordance with the manufacturer's instructions.

2.7 Transfection

The lentivirus-pHBLV-CMV-Cicr-MCS-EF1-circ_0004913, lentivirus-microRNA-1290 mimics, and their negative control were purchased from GenePharma. HCC cells were transduced with individual types of lentivirus at a multiplicity of infection (MOI) of 10 in the presence of 5 μg/ml puromycin (Thermo Fisher).

2.8 CCK-8 assay

Transfected SMCC-7721 and Huh-7 cells (1000 cells/well) were seed onto 96-well plates and incubated overnight at 37 °C. Cell proliferation was measured using the Cell Counting Kit-8 (CCK8, Dojindo, Shanghai, China) according to the manufacturer's protocol. OD values were measured at a wavelength of 450 nm using a microplate reader (Bio-Rad, CA, USA).

2.9 5-Ethynyl-2'-deoxyuridine (Edu) Assay

The EdU proliferation assay (RiboBio, Guangzhou, China) was carried out according to the manufacturer's instructions. Transfected cells were incubated with 50μM EdU for 2 h. Then an Apollo staining and DAPI staining were performed according to the instructions to detect the EdU positive cells with a fluorescence microscope.

2.10 Flow cytometric analysis

Transfected cells were suspended in 70% cold ethanol overnight after harvest. Then, cells stained with propidium iodide (PI) (Vazyme, Nanjing, China) for 30 minutes were analyzed. The proportion of cells in different cycle phases were calculated and compared.

2.11 Luciferase assay

Dual luciferase reporter system psiCHECKTM (Thermo Fisher) was used for luciferase assay. The wild type (wt) sequences and its mutant type (mut) sequences were cloned into the plasmid psiCHECK2. HEK293T cells (5×10^4 cells/well) were cultured in 24-well plates overnight and transfected with 400 ng of psiCHECK vector (psiCHECK-circ_0004913 wt, psiCHECK-circ_0004913 mut, or psiCHECK-FOXC1 wt, psiCHECK-FOXC1 mut), together with the plasmid for Renilla luciferase expression by lipofectamine 3000. One day later, the luciferase assays were performed after co-transfection with miR-1290 mimics or NC.

2.12 RNA immunoprecipitation (RIP) assay

The EZMagna RIP kit (Merck, Darmstadt, Germany) was employed for RIP assay according to the manufacturer's protocol. In brief, RIP lysis buffer was used to HEK293T cells, and the lysate products were incubated at 4 ℃ for 6 h with magnetic beads that were pre-conjugated with anti-Argonaute 2 (AGO2) or anti-IgG antibody. Afterwards, the beads were washed and digested with protease K, so as to remove the proteins. At last, the purified RNA was analyzed by qRT-PCR.

2.13 Western blot

Transfected cells were lysed in ice-cold RIPA buffer (Beyotime) with 10nM PMSF for 30 minutes and then collected to extract total protein. Total Proteins lysates were fractionated by sodium dodecyl sulfate polyacrylamide gel electrophoresis (SDS-PAGE) and then were transferred to polyvinylidene fluoride (PVDF) membrane. The membrane was blocked in 5% non-fat milk in TBST for 2h at room temperature and then immunostained overnight at 4℃ using rabbit anti-FOXC1 and PCNA (1:1000, Cell Signaling Technology, CST, USA). Rabbit anti-GAPDH (CST) was taken as a control. The signals were captured and the intensity of the bands was quantified by using the ChemiDoc XRS + system (Bio-Rad).

2.14 Mice xenograft models

For animal experiment, male BALB/c nude mice (4-6-week-old) were bought from Nanjing Medical University (Nanjing, China) and randomly divided into 2 groups (n= 5 per group). A total of 1×10^6 SMCC-7721 cells transfected with circ_0004913 or con were subcutaneously injected into mice. The tumor volume was calculated every week by the formula: length× $\text{width}^2/2$ method. After 5 weeks, the tumors were removed for subsequent experiments. This study weas approved by the Animal Committee of Affiliated Huaian No.1 People's Hospital of Nanjing Medical University.

2.15 Statistical analysis

Data were shown as Mean ± SD performed at least three independent replicates. SPSS software, 24.0 (SPSS Inc., Chicago, IL, USA) and Graphpad Prism 7.0 (San Diego, CA, USA) were used for one-way ANOVA (multiple groups), a two-tailed Student t-test (2 groups). Kaplan-Meier method test were used for survival analysis. Differences were considered as statistically significant if $P<0.05$.

3. Results

3.1 The expression of circ_0004913 was downregulated in HCC tissues and cells.

In order to study the potential role of circRNAs in the regulation of HCC process, GSE97332 and GSE94508 were selected from GEO for microarray analysis, and the expression profiles of circRNA in HCC tissues and non-tumor tissue were compared. As shown in Fig. 1A, compared with non-tumor tissues, there are 82 differentially expressed circRNAs in HCC tissues, 72 of which were up-regulated and 10 were down-regulated. According to the values of the LogFC, the top 10 dysregulated circRNAs were shown. Therefore, circ_0004913 was selected as the research object. circ_0004913, encoded by the TEX2 gene, is

located on chromosome chr17: 62248459-62265775 and about 495 bp. It was significantly reduced in the HCC tissues selected from GEO, compared with the normal tissues (Fig. 1B). Studies have confirmed the sequence of the cleavage point of the cyclization site in circ_0004913 [16] (Fig. 1C). Further analysis showed that the relative level of circ_0004913 expression in 50 HCC tissues was significantly lower than that in the adjacent liver tissues (Fig. 1D). Similarly, the relative level of circ_0004913 expression in HCC cells was significantly lower than that in L02 cells (Fig. 1E)

To further evaluate the relationship of circ_0004913 and clinical pathological features, we divided the HCC tissues into two group with circ_0004913 high expression or low expression according to circ_0004913 median expression valve. Stratified analysis showed that the lower expression of circ_0004913 was significantly associated with larger tumor size, vascular invasion, advanced TNM stage and Edmondson grade, but no other tests were performed on this population. Kaplan–Meier analysis revealed that low circ_0004913 expression also was positively associated with poor overall survival of HCC patients. Therefore, the down-regulated circ_0004913 expression may be associated with the occurrence and progression in HCC.

3.2 Circ_0004913 overexpression suppressed the proliferation of HCC cells.

Total RNA was extracted from SMCC-7721 and Huh-7 cells treated with RNase R. The expression level of linear TEX2 mRNA was significantly reduced, while the expression level of circ_0004913 did not change significantly. Thus, circ_0004913 was proved to be more stable than its linear TEX2 mRNA (Fig. 2A). As shown in Fig. 2B, nuclear and cytoplasmic mRNA grading assay was used to distinguish the subcellular localization of circ_0004913 in SMCC-7721 and Huh-7 cells, and circ_0006168 was mainly distributed in the cytoplasm. In order to study the potential function of circ_0004913 in regulating the process of HCC, we transduced the stably expressed circ_0004913 into Huh-7 and SMCC-7721 cells by using the lentivirus pHBLV-CMV-circ_0004913. After stable expression, the expression level of circ_0004913 increased significantly, while the expression level of TEX2 mRNA did not change significantly (Fig. 2C). Compared with the NC group, overexpression of circ_0004913 decreased the proliferation rate of SMCC-7721 and Huh-7 cells (Fig. 2D and 2E). To further find out the underlying mechanisms, flow cytometry was performed to analyze the correlation between cell cycle changes and circ_0004913 expression. As indicated in Fig. 2F, circ_0004417 overexpression could result in a significant increase in the percentage of HCC cells in the G1 phase. Therefore, overexpression of circ_0004913 inhibits malignant behavior by attenuating the proliferation of HCC cells.

3.3 Circ_0004913 acted as a ceRNA to sponge miR-1290.

Previous literature has shown that circRNA may serve as ceRNA to play the role of sponge miRNA, thereby reducing its inhibitory effect on targeted mRNA expression [17]. To understand the role of circRNA-0004913, we first searched for potential targeted miRNAs in the Circular RNA Interactome and circRNA Bank databases through bioinformatics. MiR-1290 may combine with circ_0004913 in the cytoplasm (Fig, 3A). Co-transfection of miR-1290 mimics and the plasmid circ_0004913 wt could significantly reduce the luciferase activity in HEK293T cells (Fig. 3B). Then, RIP assay showed that

circ_0004913 and miR-1290 were remarkably enriched in the Ago2 immunoprecipitation compared with the IgG immunoprecipitation in HEK293T cells (Fig. 3C). In addition, circ_0004913 overexpression significantly reduced the relative levels of miR-1290 in SMCC-7721 and Huh-7 cells (Fig. 3D). Compared with the adjacent liver tissue, the expression level of miR-1290 in HCC tissues were significantly increased, and it was negatively correlated with the expression level of circ_0004913 (Fig. 3E and 3F). Such data suggested that circ_0004913 may sponge miR-1290 to exert its biological function.

3.4 MiR-1290 enhanced the proliferation of HCC cells.

To investigate the role of miR-1290 in regulating the progression of HCC, we transfected miR-1290 mimics in SMCC-7721 and Huh-7 cells that with stably circ_0004913 overexpression (Fig. 4A). Compared with the control group, overexpression of miR-1290 significantly enhanced the proliferation of SMCC-7721 and Huh-7 cells and reversed the inhibitory effect of circ_0004913 on cell proliferation (Fig. 4B). Similarly, miR-1290 mimics promoted the transformation of cells from G1 phase to S phase, and accelerated cell division (Fig. 4C). Such data indicated that miR-1290 could reverse the role of circ_0004913 in cells and enhanced the malignant behaviors of HCC cells

3.5 FOXC1 may be a potential target of miR-1290.

Next, using miRDB and TargetScan to predict the potential target genes of miR-1290 through bioinformatics. Since miR-1290 enhanced the malignant behavior of HCC cells, we searched for putative target genes with tumor suppressor function. Among the potential target genes of miR-1290, FOXC1 gene was a tumor suppressor and was used as the object of this study (Fig. 5A). Further luciferase assays showed that transfection with miRNA-1290 mimics but not mutated significantly reduced FOXC1-mediated luciferase activity in HEB293T cells (Fig. 5B). After overexpressing circ_0004913, the mRNA and protein levels of FOXC1 in cells increased significantly. After transfection with miR-1290 mimics again, the expression level of FOXC1 decreased significantly (Fig. 5C and 5D).

3.6 Circ_0004913 suppressed the proliferation of HCC cells *in vivo*.

Lastly, to further confirm our conclusion *in vivo*, we performed xenograft tumor model with SMCC-7721 cells. BALB/c nude mice were monitored every three days, and euthanized in 5 weeks. By measuring tumor volume, we found that tumors from SMCC-7721 circ_0004913 cells grew slower than those from the control group (Fig. 6A, B). Similarly, tumor weight was significantly decreased in the SMCC-7721 cells inoculated with circ_0004913 overexpression (Fig. 6C). Moreover, we detected the protein levels of PCNA in xenograft tumors and found that circ_0004913 remarkably suppressed PCNA expression, indicating the inhibitory effect of circ_0004913 on HCC proliferation *in vivo* (Fig. 6D). Importantly, qRT-PCR results showed that circ_0004913 and FOXC1 expression were successfully increased, while miR-1290 expression was decreased in circ_0004913 overexpressed group in comparison to control group (Fig. 6E, F).Taken together, these results suggest that circ_0004913 inhibits tumor growth *in vivo,* consistent with our data *in vitro.*

4. Discussion

Our research indicated that circ_0004913 acted as a tumor suppressor through the miR-1290/FOXC1 axis to inhibit HCC cancer cell proliferation, suggesting that circ_0004913 may be a potential biotherapeutic target for HCC. Our findings supported: (1) circ_0004913 was down-regulated in HCC tissues and HCC cell lines, which was positively associated with poor clinical pathological features and overall survival of HCC patients; (2) circ_0004913 could delay the cell cycle progression of HCC cell lines and decrease the rate of cell proliferation; (4) circ_0004913 was a miR-1290 sponge, and circ_0004913 overexpression could significantly inhibit cell growth; (5) circ_0004913 sponged miR-1290 to promote FOXC1 expression and was necessary to regulate cancer progression. Therefore, our study identified the previously unknown role of circ_0004913 in inhibiting the occurrence and development of HCC.

Circ_0004913 is derived from TEX2. In this study, circ_0004913 was down-regulated in HCC tissue samples and cell lines, which is consistent with the results from other institutions. Lower expression of circ_0004913 was significantly associated with high level of AFP, history of liver cirrhosis, larger tumors, and distant metastases. Previous studies have shown that circRNAs could play a crucial role in cell cycle progression and proliferation [18, 19]. After RNase R treatment, circ_0004913 was still detected with a little degradation. We provided evidence that ectopic expression of circ_0004913 could delay the cycle progression of HCC cells. These results indicated that circ_0004913 was closely related to the malignant progression of HCC.

Although the mechanism through which circRNA regulates carcinogenesis and cancer progression has not yet been fully elucidated, the "circRNA-miRNA-mRNA" axis, also known as the "miRNA sponge", has shown its potentiality [20]. In our research, we confirmed that the content of circ_0004913 in the cytoplasm was significantly higher than that in the nucleus, which also provides a basis for circ_0004913 to sponge miRNAs [21]. Circ_0004913 may be a miR-1290 sponge. miR-1290 has been reported to show a high expression in the tissues and blood of various cancer patients [22-25]. For example, miR-1290 promote colorectal cancer cell proliferation by targeting INPP4B and accelerated the metastasis of oral squamous cell carcinoma by inhibiting CCNG2 expression [23, 26]. miR-1290 was also highly expressed in the plasma of cancer patients, and has the potential to be a tumor marker and to guide the prognosis of patients [27-29].We hypothesized that overexpression of circ_0004913 could significantly reduce the expression of miR-1290, thereby inhibiting the proliferation, migration and invasion of HCC cell lines. We confirmed the direct correlation between miR-1290 and circ_0004913 through dual luciferase assay and RIP assay. MiR-1290 was significantly upregulated in HCC cells and tissues, and its overexpression promoted cell proliferation and accelerated cell transformation from G0/G1 phase to S phase. Therefore, an increase in circ_0004913 expression in HCC cells leads to a decrease in miR-1290 expression, thereby inhibiting proliferation and cell cycle progression. Our results provided evidence that miR-1290 sponge caused by circ_004913 drives HCC progression, and circ_0004913 is the upstream target of miR-1290.

Next, through bioinformatics and luciferase reporter gene analyses, we confirmed that the target gene of circ_004913/miR-1290 was FOXC1. A large number of latest data indicated that FOXC1 was involved in

the development of cancers, including HCC, and FOXC1 played a inhibitory role in the proliferation, migration, invasion and metastasis of HCC cells [30, 31]. It has been shown that overexpression of FOXC1 in HCC cells inhibits epithelial to mesenchymal transformation, migration and invasion *in vitro* [32]. We additionally revealed that circ_0004913/miR-1290 regulated FOXC1, as part of the sponge mechanism. Increasing circ_0004913 expression promoted FOXC1 expression, while increasing miR-1290 expression inhibited FOXC1 expression. To our knowledge, our study is the first to prove that circ_0004913 is involved in FOXC1 expression. These findings indicated that circ_0004913 protect FOXC1 from miR-1290-mediated degradation in a competitive endogenous RNA-mediated manner.

We admitted that our research still has limitations. circRNA may rely on other mechanisms in the occurrence and development of HCC. The role of circ_0004913 in HCC remains to be explored. We still need to carry out experiments with larger sample size to evaluate the expression stability of circ_0004913 in peripheral blood of patients with liver cancer.

Conclusion

Circ_0004913 was significantly down-regulated in HCC tissues and cell lines. The up-regulation of circ_0004913 significantly inhibited the proliferation and cycle progression of HCC cells. Circ_0004913 sponged miR-1290 to regulate FOXC1 expression. Therefore, circ_0004913 could be used as a promising prognostic biomarker and a therapeutic target for HCC patients.

Abbreviations

CircRNAs: Circular RNAs; HCC: Hepatocellular carcinoma; GEO: Gene Expression Omnibus database; qRT-PCR: Quantitative reverse transcription PCR; FOXC1:Forkhead box C1; TEX2: Testis expressed 2; HBV: Chronic hepatitis B virus; HCV: Hepatitis C virus; miRNAs: microRNAs; CCK8:Cell Counting Kit-8; Edu: 5-Ethynyl-2’-deoxyuridine; RIP: RNA immunoprecipitation.

Declarations

Acknowledgements

None

Authors' contributions

Conception and design: YYB, QFZ. Development of methodology: HSY. Acquisition of data: SY. Analysis and interpretation of data: LM. Writing, review, and revision of article: YYB. All authors read and approved the final manuscript.

Funding

This work was supported by the Scientific development funding of Nanjing medical university (NMUB2018259).

Consent for publication

All authors approved publication of the manuscript.

Competing interests

None

Competing interests

The authors declare that they have no financial conflicts of interest.

Ethics approval and consent to participate

This study was authorized by the Ethics Committee of Huaian No.1 People's Hospital; all animal procedures were approved by the Animal Committee of Affiliated Huaian No.1 People's Hospital of Nanjing Medical University (IACUC-1906548).

Data availability

All data generated during this study are included in this published article.

References

1. Bray, F., et al., *Global cancer statistics 2018: GLOBOCAN estimates of incidence and mortality worldwide for 36 cancers in 185 countries.* CA Cancer J Clin, 2018. **68**(6): p. 394-424.
2. Kulik, L. and H.B. El-Serag, *Epidemiology and Management of Hepatocellular Carcinoma.* Gastroenterology, 2019. **156**(2): p. 477-491.e1.
3. Singal, A.G. and H.B. El-Serag, *Hepatocellular Carcinoma From Epidemiology to Prevention: Translating Knowledge into Practice.* Clin Gastroenterol Hepatol, 2015. **13**(12): p. 2140-51.
4. Grandhi, M.S., et al., *Hepatocellular carcinoma: From diagnosis to treatment.* Surg Oncol, 2016. **25**(2): p. 74-85.
5. Nishida, N. and M. Kudo, *Oncogenic Signal and Tumor Microenvironment in Hepatocellular Carcinoma.* Oncology, 2017. **93 Suppl 1**: p. 160-164.
6. Greene, J., et al., *Circular RNAs: Biogenesis, Function and Role in Human Diseases.* Front Mol Biosci, 2017. **4**: p. 38.
7. Tang, Q. and S.S. Hann, *Biological Roles and Mechanisms of Circular RNA in Human Cancers.* Onco Targets Ther, 2020. **13**: p. 2067-2092.

8. Lu, C., et al., *Knockdown of circular RNA circ-FARSA restricts colorectal cancer cell growth through regulation of miR-330-5p/LASP1 axis.* Arch Biochem Biophys, 2020: p. 108434.
9. Dong, L. and F. Qu, *CircUBAP2 promotes SEMA6D expression to enhance the cisplatin resistance in osteosarcoma through sponging miR-506-3p by activating Wnt/β-catenin signaling pathway.* J Mol Histol, 2020.
10. Chen, L.L., *The biogenesis and emerging roles of circular RNAs.* Nat Rev Mol Cell Biol, 2016. **17**(4): p. 205-11.
11. Li, R., S. Luo, and D. Zhang, *Circular RNA hsa_circ_0054537 sponges miR-130a-3p to promote the progression of Renal Cell Carcinoma through regulating cMet pathway.* Gene, 2020: p. 144811.
12. Chen, L., et al., *Circ_0008532 promotes bladder cancer progression by regulation of the miR-155-5p/miR-330-5p/MTGR1 axis.* J Exp Clin Cancer Res, 2020. **39**(1): p. 94.
13. Aghaee-Bakhtiari, S.H., *Online Databases and Circular RNAs.* Adv Exp Med Biol, 2018. **1087**: p. 35-38.
14. Han, D., et al., *Circular RNA circMTO1 acts as the sponge of microRNA-9 to suppress hepatocellular carcinoma progression.* Hepatology, 2017. **66**(4): p. 1151-1164.
15. Fu, L., et al., *Screening differential circular RNA expression profiles reveals hsa_circ_0004018 is associated with hepatocellular carcinoma.* Oncotarget, 2017. **8**(35): p. 58405-58416.
16. Xiong, D.D., et al., *A circRNA-miRNA-mRNA network identification for exploring underlying pathogenesis and therapy strategy of hepatocellular carcinoma.* J Transl Med, 2018. **16**(1): p. 220.
17. He, Y., et al., *CircZNF609 enhances hepatocellular carcinoma cell proliferation, metastasis, and stemness by activating the Hedgehog pathway through the regulation of miR-15a-5p/15b-5p and GLI2 expressions.* Cell Death Dis, 2020. **11**(5): p. 358.
18. Wang, Y., et al., *Circular RNA hsa_circ_0003141 promotes tumorigenesis of hepatocellular carcinoma via a miR-1827/UBAP2 axis.* Aging (Albany NY), 2020. **12**.
19. Wang, M., F. Yu, and P. Li, *Circular RNAs: Characteristics, Function and Clinical Significance in Hepatocellular Carcinoma.* Cancers (Basel), 2018. **10**(8).
20. Kulcheski, F.R., A.P. Christoff, and R. Margis, *Circular RNAs are miRNA sponges and can be used as a new class of biomarker.* J Biotechnol, 2016. **238**: p. 42-51.
21. Huang, J., et al., *Exosome-mediated transfer of miR-1290 promotes cell proliferation and invasion in gastric cancer via NKD1.* Acta Biochim Biophys Sin (Shanghai), 2019. **51**(9): p. 900-907.
22. Qin, W.J., et al., *MiR-1290 targets CCNG2 to promote the metastasis of oral squamous cell carcinoma.* Eur Rev Med Pharmacol Sci, 2019. **23**(23): p. 10332-10342.
23. Sun, Y., et al., *miR-1290 promotes proliferation and suppresses apoptosis in acute myeloid leukemia by targeting FOXG1/SOCS3.* J Biol Regul Homeost Agents, 2019. **33**(6): p. 1703-1713.
24. Wei, J., et al., *Serum miR-1290 and miR-1246 as Potential Diagnostic Biomarkers of Human Pancreatic Cancer.* J Cancer, 2020. **11**(6): p. 1325-1333.
25. Xia, L., et al., *Overexpression of forkhead box C1 promotes tumor metastasis and indicates poor prognosis in hepatocellular carcinoma.* Hepatology, 2013. **57**(2): p. 610-24.

26. Xu, Z., et al., *C/EBPα Regulates FOXC1 to Modulate Tumor Growth by Interacting with PPARγ in Hepatocellular Carcinoma.* Curr Cancer Drug Targets, 2020. **20**(1): p. 59-66.
27. Xu, Z.Y., et al., *FOXC1 contributes to microvascular invasion in primary hepatocellular carcinoma via regulating epithelial-mesenchymal transition.* Int J Biol Sci, 2012. **8**(8): p. 1130-41.

Figures

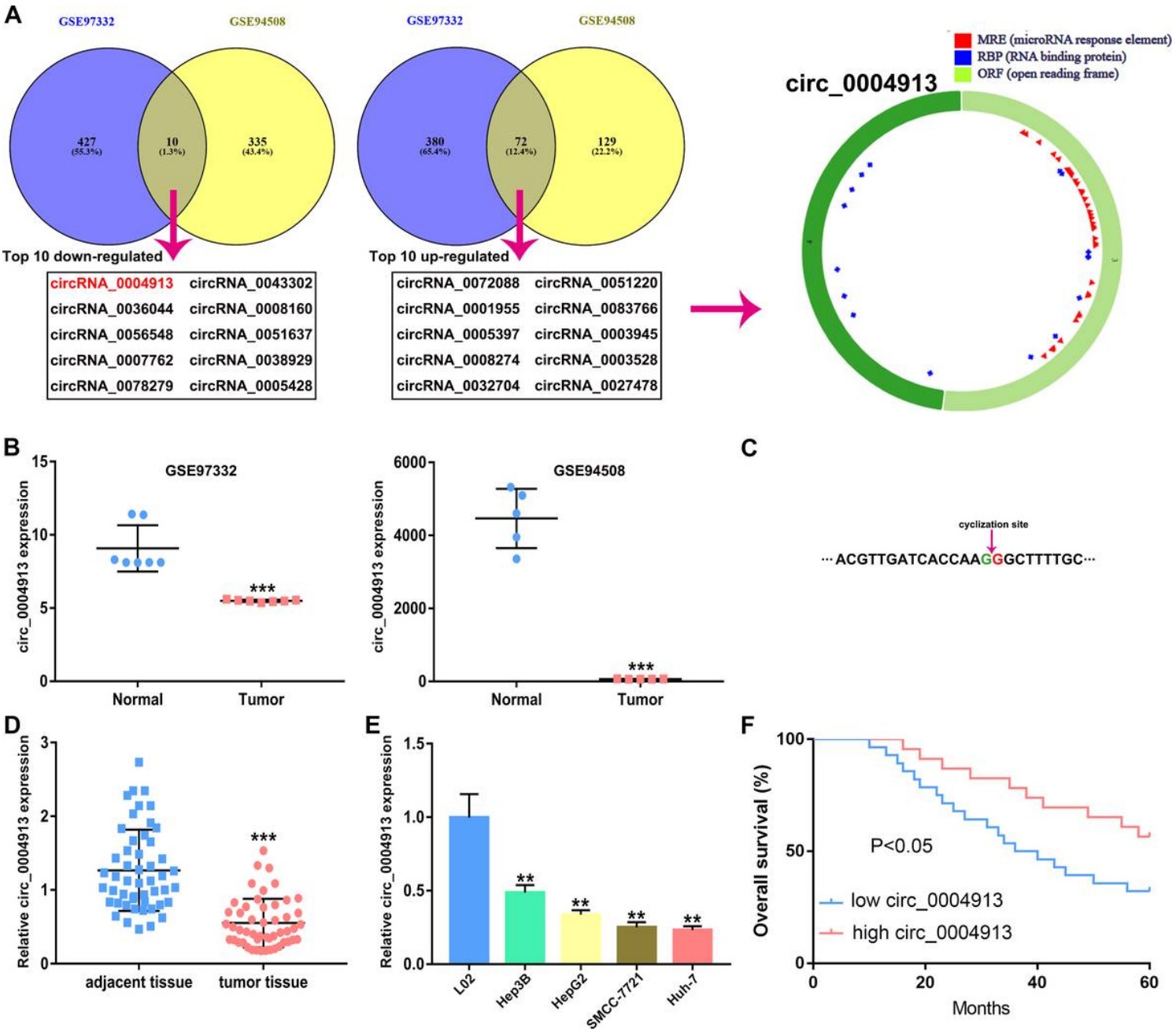

Figure 1

circ_0004913was lowly expressed in HCC tissue and cells. A. GSE79332 and GSE94508 unveiled dysregulated circRNAs in the HCC tissues, and circ_0004913 was chosen as a study object. B. circ_0004913 expression in GSE97332 and GSE94508. C. The existence of hsa_circ_0006168 and its

cyclization site (red arrow). D. Relative circ_0004913 expression in HCC tissues and adjacent tissues. E. Relative circ_0004193 expression in HCC cells and L02. Data (n=5) are the means ± SD. *P <0 .05, **P <0 .01, ***P <0 .001.

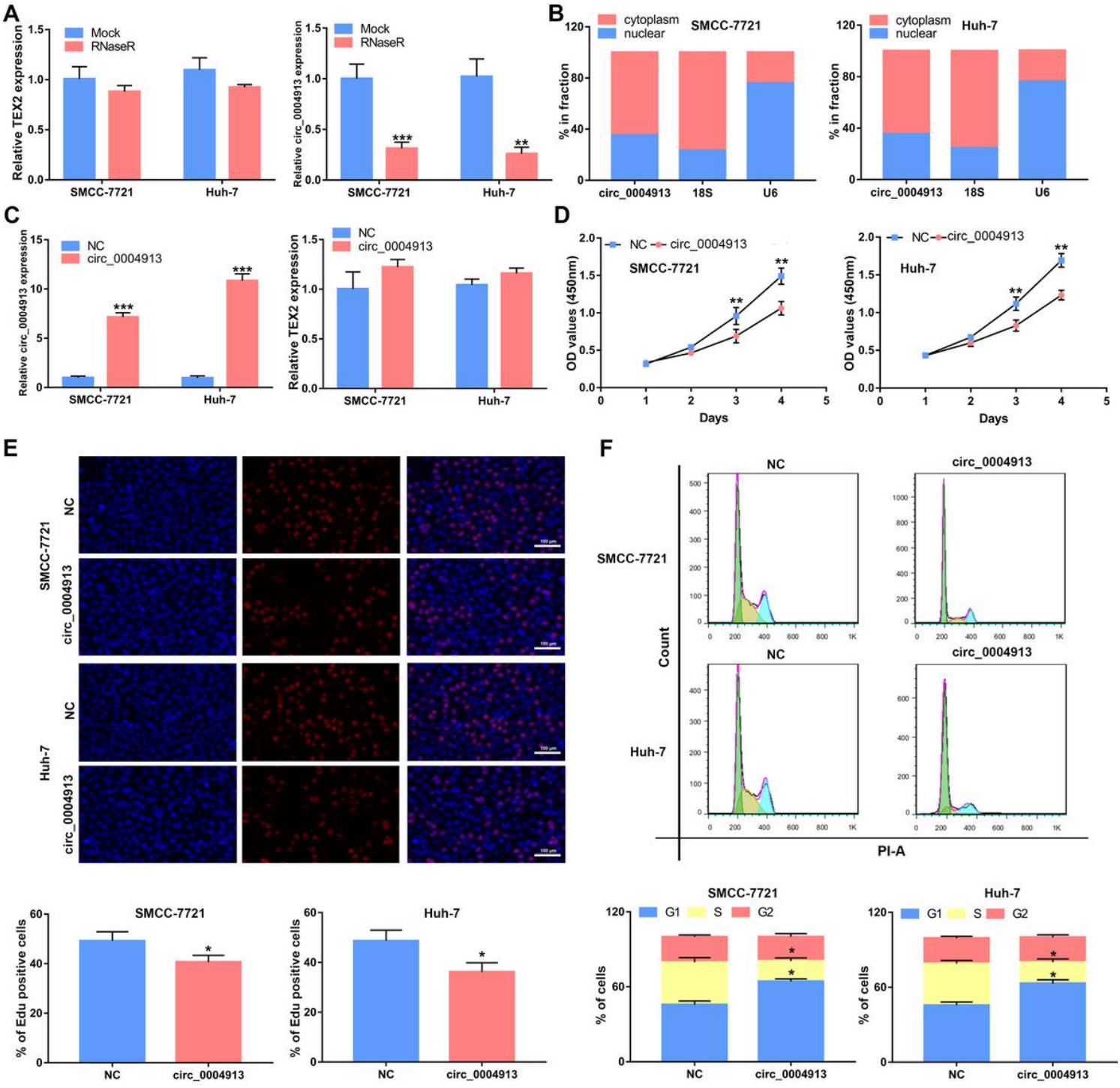

Figure 2

circ_0004913 affected proliferation and cell cycle of HCC cells. A, After RNase R treatment, circ_0004913 expression level and TEX2 mRNA expression level in SMCC-7721 and Huh-7 cells were measured. B. Nuclear and cytoplasmic mRNA fraction experiment displays the location of circ_0004913 in SMCC-7721 and Huh-7 cells. C. The expression levels of circ_0004913 and TEX2 in transfected SMCC-7721 and Huh-

7 cells. D. The proliferation capacities of transfected SMCC-7721 and Huh-7 cells were detected by CCK-8 assays. E. The proliferation capacities of transfected SMCC-7721 and Huh-7 cells were detected by Edu assays. F, Flow cytometry analysis revealed the cycle arrest of transfected SMCC-7721 and Huh-7 cells. Data (n=5) are the means ± SD. *P <0 .05, **P <0 .01, ***P <0 .001.

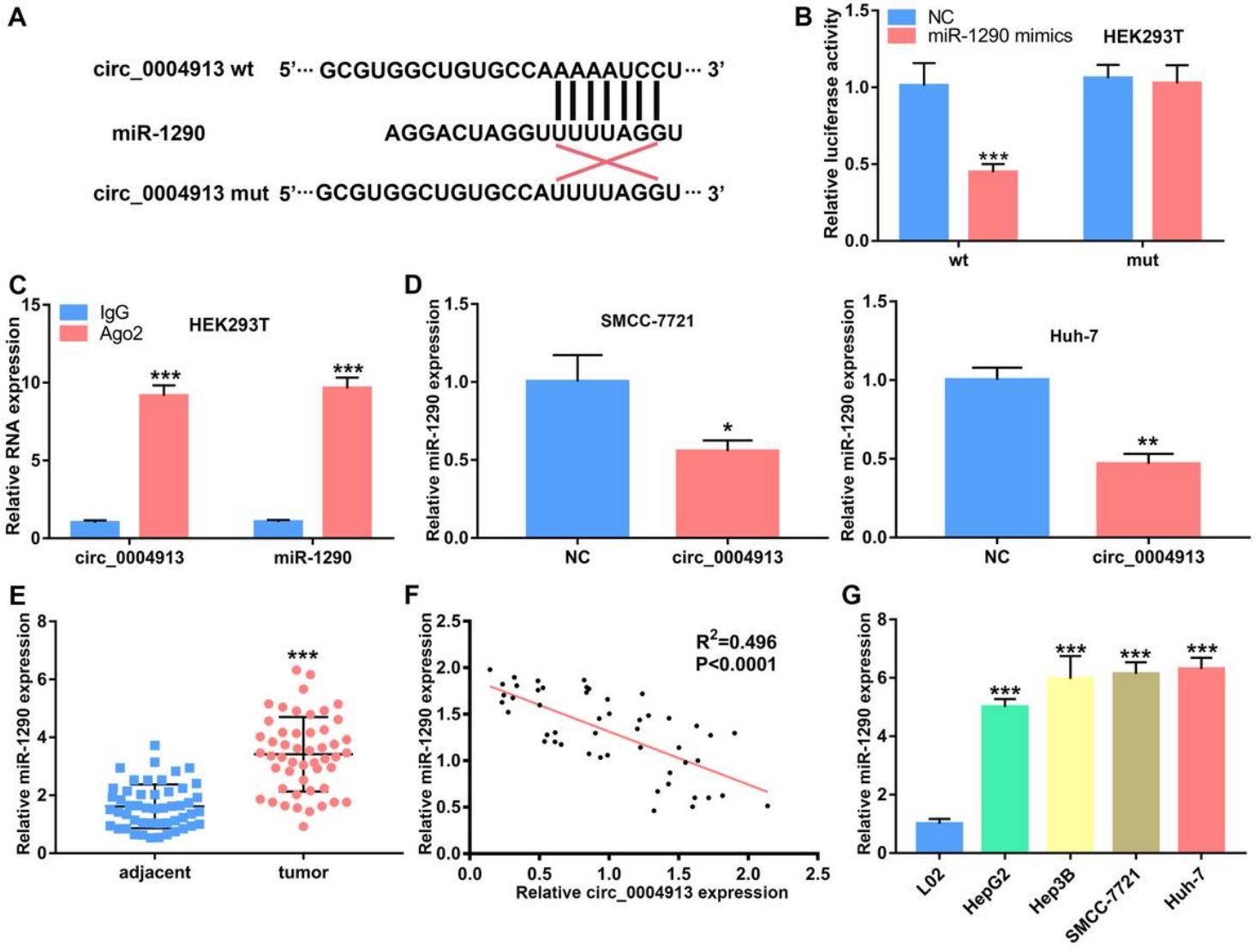

Figure 3

miR-1290 acted as the target of circ_0004913. A. Bioinformatics tools indicated the complementary binding sites of miR-1290 with circ_0004913. B. Luciferase reporter assay showed the targeting of miR-1290 with circ_0004913 in HEK293T C. RIP and qRT-PCR assays measured the expression differences in circ_0004913 and miR-1290 between the Ago2 immunoprecipitation and the IgG immunoprecipitation. D. qRT-PCR showed the miR-1290 expression after circ_0004913 overexpression. E. Relative miR-1290 expression in HCC tissues and adjacent tissues. F. The correlation between miR-605 and circFBXO11 was calculated by Spearman's rank correlation coefficients. G. Relative miR-1290 expression in HCC cells and L02. Data (n=5) are the means ± SD. *P <0 .05, **P <0 .01, ***P <0 .001.

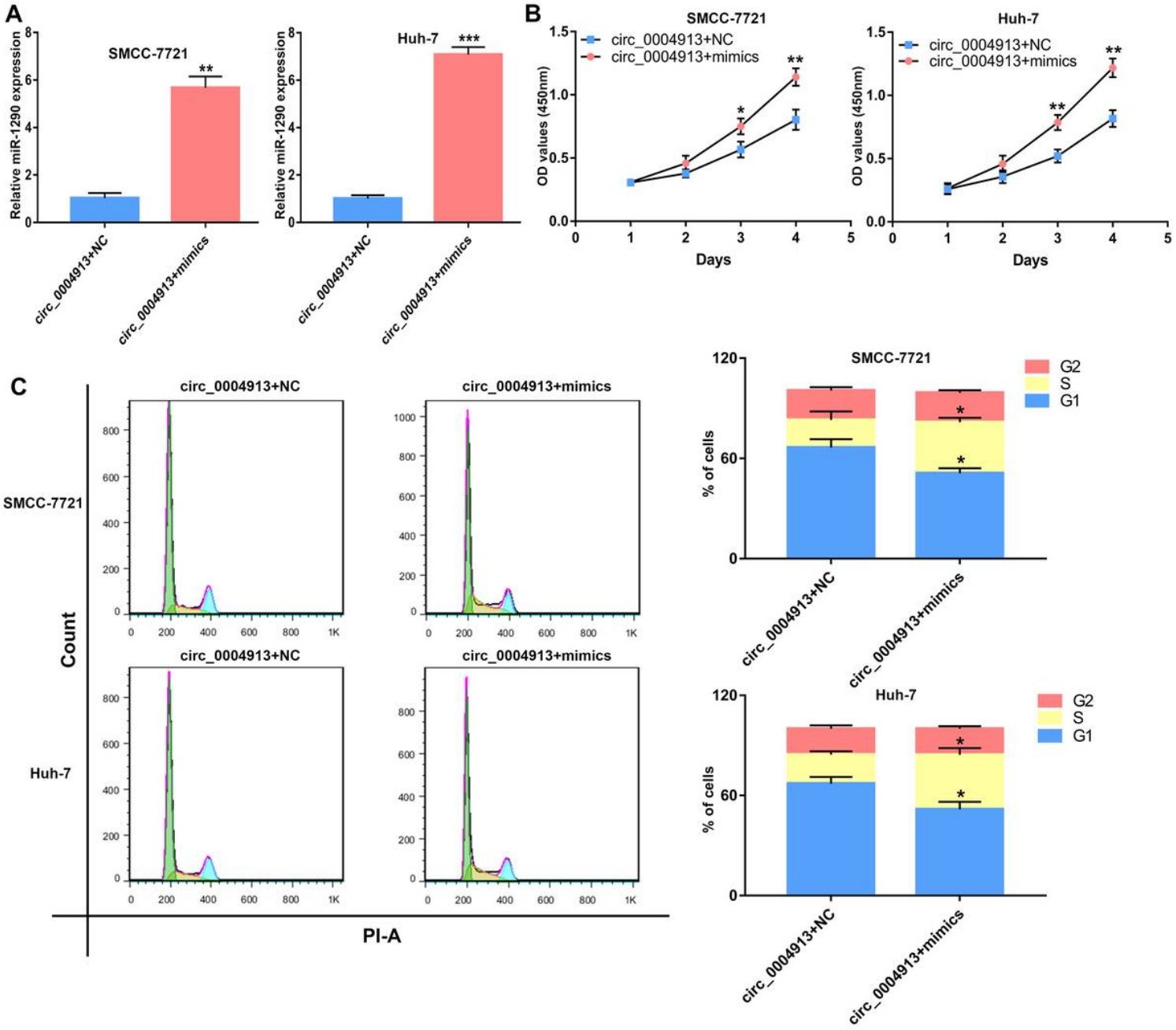

Figure 4

miR-1290 promoted cell proliferation in HCC cells. A. Relative miR-1290 expression in transfected cells. B. The proliferation capacities of transfected SMCC-7721 and Huh-7 cells were detected by CCK-8 assays. C. The proliferation capacities of transfected SMCC-7721 and Huh-7 cells were detected by Edu assays. Data(n=5) are the means ± SD. *P <0 .05, **P <0 .01, ***P <0 .001.

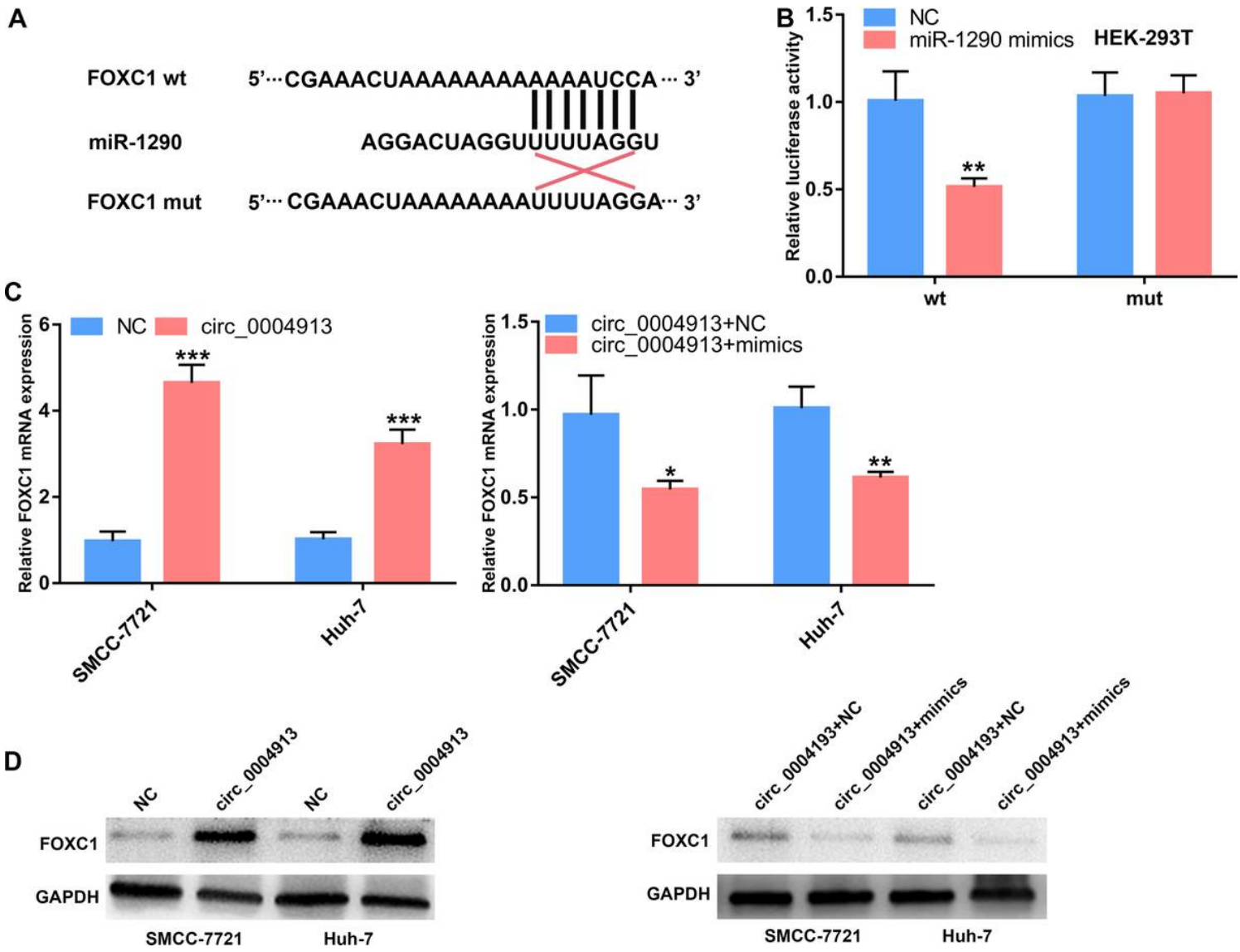

Figure 5

circ_0004913 regulated miR-1290/FOXC1 axis. A. Bioinformatics tools indicated the complementary binding sites of miR-1290 with FOXC1. B. Luciferase reporter assay showed the targeting of miR-1290 with FOXC1 in HEK293T. C. qRT-PCR showed the FOXC1 mRNA expression in transfected SMCC-7721 and Huh-7 cells. D. Western blot showed the FOXC1 protein expression in transfected cells. Data(n=5) are the means ± SD. *P <0 .05, **P <0 .01, ***P <0 .001.

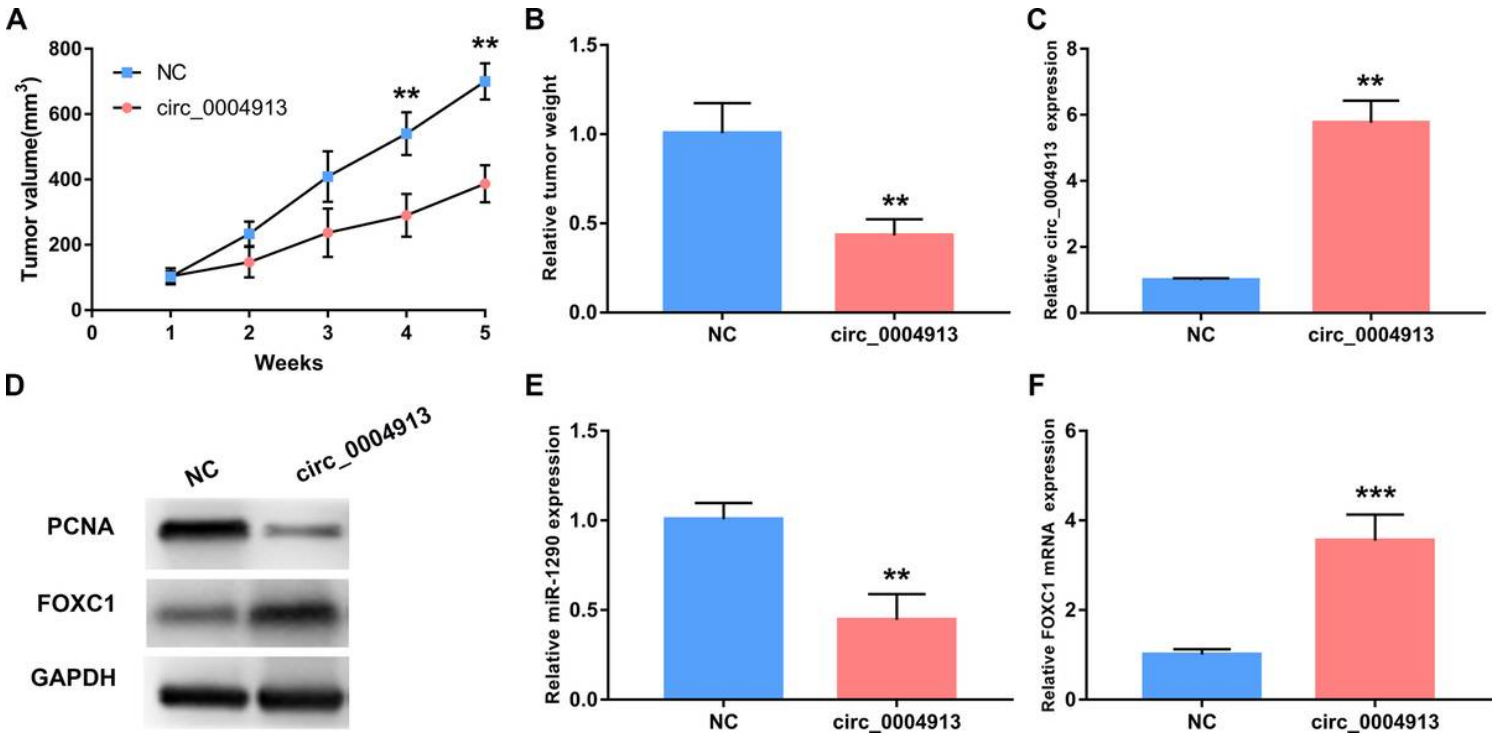

Figure 6

circ_0004913 suppressed the proliferation of HCC cells in vivo. A. Tumor volume was calculated with length× width2/2 method at the indicated time point. B. The image of xenograft tumor in control or circ-1004913 group (n=3/group, Scale bar= 1 cm.). C. Tumor weight was measured in mice. D. The expression level of circ_1004913 was detected by qRT-PCR. E. The protein levels of PCNA and FOXC1 were tested by WB analysis. F, G. qRT-PCR analysis of miR-1290 and FOXC1 expression in nude mice bearing xenograft tumor with or without circ_0004913 overexpression. Data(n=5) are the means ± SD. *P <0 .05, **P <0 .01, ***P <0 .001.